Crystallization of *s*-Polypropylene from the Glassy State: Indications for a Multistage Process

M. Grasruck* and G. Strobl

Fakultät für Physik, Albert-Ludwigs-Universität, 79104 Freiburg, Germany

Received July 8, 2002; Revised Manuscript Received October 18, 2002

ABSTRACT: Annealing of sPP after a rapid quench from the melt to a temperature below T_g (−3 °C) leads for an annealing temperature $T_c = 0$ °C to a trans-rich mesomorphic phase, for $T_c = 25$ °C to the helical crystalline phase, and for $T_c = 2$ °C to a mixture of both phases. SAXS experiments show that the layer thickness and the long spacing are always the same; i.e., they are independent of the inner structure of the lamellae. This can be understood as indicating that the crystals form only in a second step, subsequent to an initial formation of mesomorphic layers.

Introduction

If syndiotactic polypropylene (sPP) is crystallized from the amorphous glassy state, peculiarities arise. This was at first observed by Nakaoki, Ohira, and Horii[1,2] and then again with some modifications in the interpretation by Guadagno, Vittoria, and de Rosa et al.[3−5] It is found that samples kept for sufficiently long time, on the order of some hours, at 0 °C will not crystallize when they are subsequently stored at room temperature. The effect disappears, i.e., samples *do* crystallize at room temperature if the melt after a quench to 0 °C, which is near T_g (−3 °C), is brought up immediately to 25 °C. The reason for the difference in behavior showed up in NMR and IR spectra as well as in wide-angle X-ray scattering (WAXS) experiments: During a prolonged storage at 0 °C a mesomorphic phase with a high content of chains in the trans-planar modification forms, and its presence then suppresses the formation of the helical crystalline form (modifications I and II of sPP) at room temperature. On drawing samples, both the trans-planar mesomorphic and the helical crystalline forms turn into the trans-crystalline modification (modification III); on releasing the load, however, they transform back into the different initial states.[3] Irreversible changes follow from a heating. Beginning around 60 °C, a transformation from the trans-planar mesomorphic to the crystalline phase is observed. This transformation is irreversible; i.e., the mesomorphic phase is not reestablished on cooling.

We now have studied this process applying time- and temperature-dependent simultaneous small- and wide-angle X-ray scattering experiments, complemented by dilatometry. Our results indicate that the crystallization of sPP from the glassy state always, i.e., independent of the time of storage at 0 °C, passes through a mesomorphic phase—the trans-planar mesomorphic or another one —as an intermediate.

Experimental Section

Samples. Two different samples of sPP were used in the studies. The first, called sPP-F, is a commercial brand obtained by FINA Oil, Brussels. It has 83% syndiotactic pentades and a molar mass $M_w = 6 \times 10^4$ g mol^{-1} ($M_w/M_n = 4$). The second sample, called sPP-M, was synthesized in the Institute of Macromolecular Chemistry of our university and has a higher tacticity, corresponding to 92% of syndiotactic pentades, as was derived from the NMR spectrum.

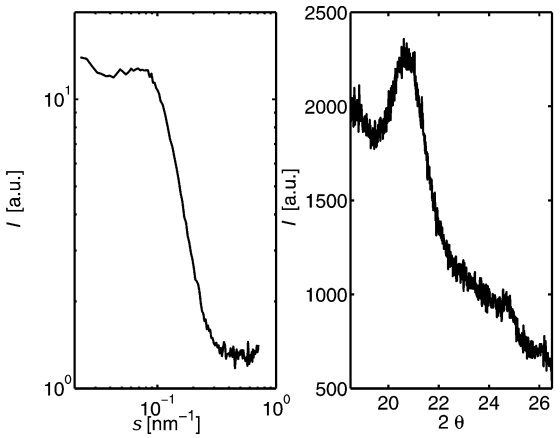

Figure 1. Data obtained with the aid of the twin small-angle/wide-angle X-ray scattering camera for sPP-F crystallized at 25 °C after a quench in ice water: (left) slit-smeared SAXS curve showing a long spacing peak ($s = 2 \sin \theta/\lambda$ with θ denoting the Bragg angle); (right) WAXS curve with the 121 Bragg reflection.

Simultaneous Small- and Wide-Angle X-ray Scattering. The X-ray scattering experiments were carried out with the aid of a twin camera produced by Hecus-M.Braun Co., Graz, Austria. In this device a Kratky small angle camera is complemented by a second camera set on top of it which simultaneously registers the X-ray scattering in the angular range $2\theta = 19°-26°$ (θ: Bragg scattering angle). Small-angle X-ray scattering (SAXS) and WAXS are registered separately, employing two one-dimensional position-sensitive wire detectors. The intensity data obtained are stored and further evaluated in a PC. We used a Cu anode, fabricated by Bruker AXS, Karlsruhe, Germany, as an X-ray source, together with a Ni filter to extract the Kα radiation. Figure 1 shows as an example typical results obtained for sPP in the semicrystalline state. The left side gives the slit-smeared SAXS curve and the right side the WAXS pattern. The pattern includes a strong reflection at $2\theta = 21.7°$ and two more, although much weaker reflections, above 24°, all of them belonging to the helical crystalline form of sPP. The strong reflection is the 121

* Corresponding author.

10.1021/ma021074t CCC: $25.00
Published on Web 12/12/2002

reflection, superposed on the low angle side by the weaker 220 reflection; the two weak reflections are to be assigned to 002 and 400 (*hkl*), respectively.

Evaluation of SAXS Data. Having determined the primary beam intensity with the aid of a moving slit system, desmeared scattering curves were obtained in absolute values, as differential cross sections per unit volume $\Sigma(q)$. With a knowledge of $\Sigma(q)$ the one-dimensional electron density autocorrelation function $K(z)$ and its second derivative $K''(z)$, which gives the interface distance distribution function (IDF),[6,7] can be directly calculated by applying the Fourier relations

$$K(z) = \frac{1}{r_e^2}\frac{1}{(2\pi)^3}\int_0^\infty \cos qz\ 4\pi q^2\Sigma(q)\ \mathrm{d}q \tag{1}$$

and

$$K''(z) = \frac{2}{r_e^2(2\pi)^2}\int_0^\infty [\lim_{q\to\infty} q^4\Sigma(q) - q^4\Sigma(q)] \cos qz\ \mathrm{d}q \tag{2}$$

Here, q denotes the scattering vector $q = 2\pi s = 4\pi \sin\theta/\lambda$; r_e is the classical electron radius. In all the measurements the crystal thickness d_c was derived from the location of the respective peak in $K''(z)$.

A useful parameter in kinetic measurements and also the analysis of the continuous melting on heating is the Porod coefficient. It generally describes for two-phase systems the asymptotic behavior of the scattering curve as

$$\lim_{q\to\infty} \Sigma(q) = r_e^2 \frac{P}{(q/2\pi)^4} \tag{3}$$

The Porod coefficient P is directly related to the interface area per unit volume, O_{ac}, by

$$P = \frac{1}{8\pi^3} O_{ac}(\Delta\rho)^2 \tag{4}$$

whereby $\Delta\rho$ denotes the difference in the electron densities of the two phases. This relation is generally valid for homogeneous as well as heterogeneous structures and therefore, for example, also if spherulites or other objects fill a sample only partially.

Determination of Bragg Reflection Intensities. The aim of the WAXS experiments was the determination of the intensities of Bragg reflections during structure-evolution and -modification processes, as they take place during isothermal crystallizations and subsequent heatings. To optimize the measurement's sensitivity, we chose the 121 reflection, which has the highest intensity. In a first step the WAXS curve of the melt—extrapolated to the crystallization temperature in order to account for the temperature shift of the halo and adjusted to the measured curve—was subtracted from the data. Then the integral intensity from the peak location to higher angles was determined.

As it turned out in the various measurements, there exists a point in the WAXS curve where crystals and the amorphous phase produce equal scattering intensities. This invariant intensity can be used as an inner standard. Referring to it eliminates possible fluctuations of the primary beam intensity and enables also comparisons to be drawn between different samples where the thicknesses may vary. All the WAXS intensity data were correspondingly referred to a common, conveniently chosen value of this inner standard.

The SWAXS Ratio. Small-angle X-ray scattering generally arises if densified regions with mesoscopic lengths exist in a sample, whereas Bragg reflections in the WAXS pattern occur only if crystals exist. If the densification of a polymer after cooling a melt takes place associated with the formation of crystal lamellae only, the development of scattering in the small angle range and the scattering in the wide angle range

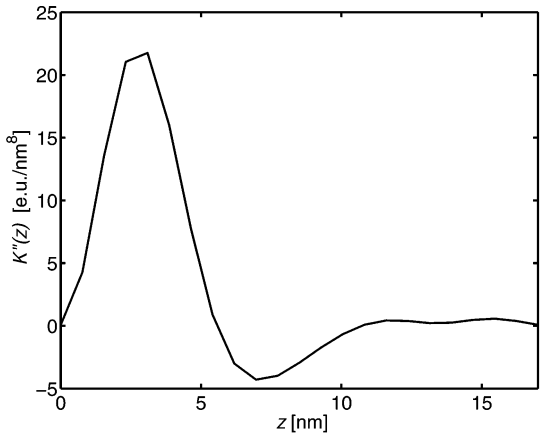

Figure 2. sPP-F crystallized at 25 °C after a quench of the melt in ice water: Interface distance distribution function derived from the SAXS data shown in Figure 1.

are directly related. More accurately, crystallinities may be derived from both SAXS and WAXS according to

$$\phi(\mathrm{WAXS}) \sim I \tag{5}$$

and

$$\phi(\mathrm{SAXS}) = \frac{O_{ac}d_c}{2} \sim Pd_c \tag{6}$$

If the densification is due to the crystal formation only, both should agree, and the parameter

$$\alpha = \frac{I}{Pd_c} \tag{7}$$

addressed in the following as SWAXS ratio should be constant throughout an isothermal structure formation process. Since

$$P \sim (\Delta\rho)^2 \tag{8}$$

one expects during a heating with unchanged crystallinity a continuous, smooth uprise of α because $\Delta\rho$ increases with temperature. On the other hand, if the densification during the structure formation process is achieved by the growth of noncrystalline or partially crystalline layers or of imperfect crystals, deviations in the value of the SWAXS ratio occur.

Atomic Force Microscopy. For AFM observation we used a Nanoscope III. We thereby employed the tapping technique, thus probing the viscoelastic properties of lamellar surfaces and edges. Height-amplitude and phase mode yielded consistent results with the better contrast in the phase mode. The necessary planarity of the surface was achieved by first preparing a thin film from solution which was subsequently isothermally crystallized.

Dilatometry. The structure formation in a first glassy amorphous sample at 0 °C was also studied with the aid of a mercury-filled dilatometer. Absolute values of the change in the specific volume were obtained after a calibration.

Results

Figure 2 presents the interface distance distribution function derived from the SAXS data of Figure 1. These data were obtained for a sample that was quenched from the melt in ice−water, kept there only shortly (1 min), and then brought to room temperature where the crystallization took place. Under these conditions the kinetics is too rapid to be resolved in time-dependent measurements. The scattering curve of Figure 1 and the derived interface distribution function represent there-

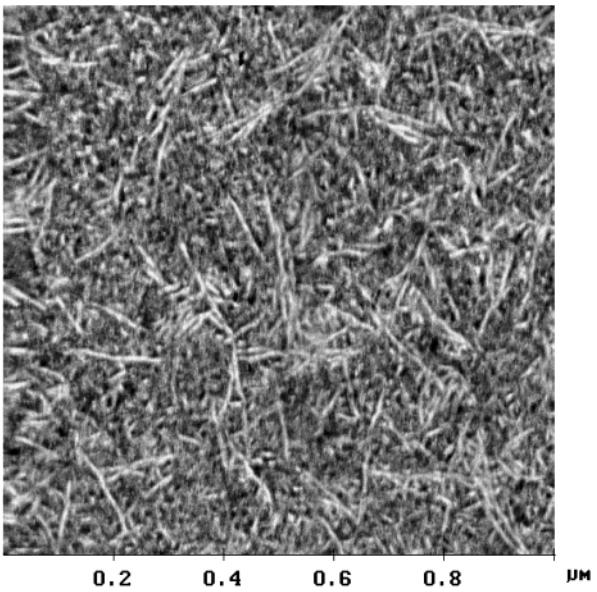

Figure 3. Tapping mode AFM image of a sample cold crystallized at room temperature.

fore the final state reached after completion of the structure formation process.

Before calculating the (one-dimensional) interface distance distribution function, one to be sure that the sample under study has a lamellar structure. The best means to obtain this knowledge is the use of the AFM. Figure 3 displays images of the semicrystalline structure developed at room temperature after the short quench. As is obvious, layers, although not planar over very large lateral distances, do exist. We therefore can put trust into structure parameters derived from the SAXS curve. From the IDF we can take the crystal thickness, which is $d_c = 2.8$ nm. The value of the Porod coefficient amounts to $P = 0.44$ eu nm^{-7}. For the long spacing we obtained $L = 8.3$ nm. The (linear) crystallinity d_c/L following from the data amounts to 32%. In previous work on sPPs with different tacticity and syndiotactic poly(propylene−octene) copolymers we have measured the thicknesses of crystals as they form at different crystallization temperatures T_c.[8] When plotting the inverse of the crystal thickness d_c^{-1} vs T_c all results fall onto a common line, addressed by us as the crystallization line of sPP.[9] Figure 4 shows this crystallization line together with the new results obtained by crystallizing samples from the glassy state. The point corresponding to $d_c = 2.8$ nm for $T_c = 25$ °C is included as a filled circle. As we see, within the error limits of the measurement also this point is located on the crystallization line. That the intermediate short quench to the glassy state does not change the mechanism of crystallization is an expected result. Of interest, however, is the observation that, with the additional point included, the equation

$$d_c = \frac{472 \text{ K nm}}{469 \text{ K} - T_c} \tag{9}$$

which describes the crystallization line now holds over the large temperature range of 200 °C.

Figure 5 now presents in a 3-dimensional manner the result of a SWAXS experiment carried out for a sample which after the quench was kept in ice−water to solidify at this temperature. The change of the SAXS curve with

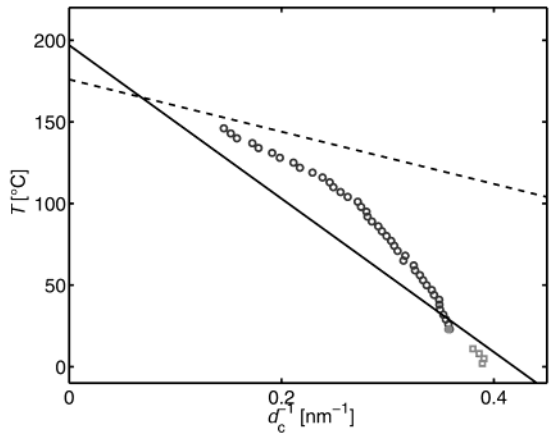

Figure 4. Crystal thicknesses measured at various temperatures. sPP-M cold crystallized at 25 °C (bullet); changes with temperature during a subsequent heating (circle); sPP-F solidified at 2, 5, 8, and 11 °C (square). Crystallization line and Gibbs−Thomson melting line obtained previously[10] for a sample similar to sPP-M, which was isothermally crystallized from the melt.

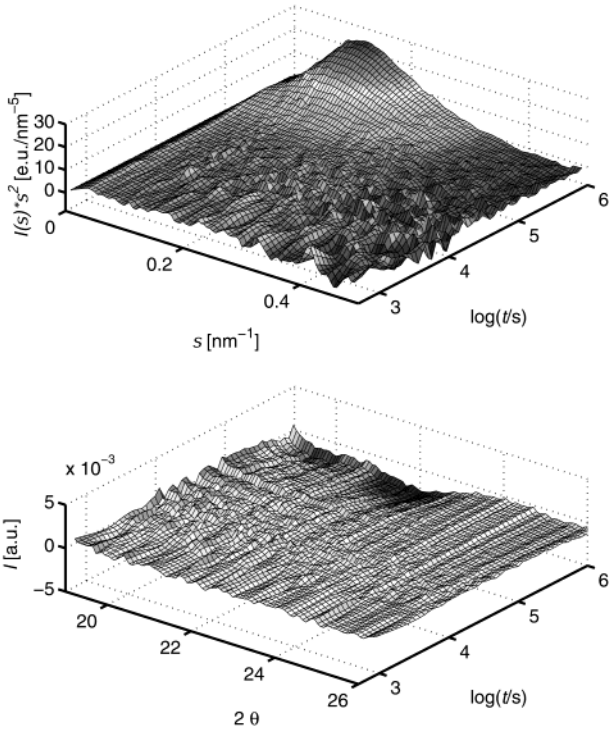

Figure 5. sPP-M: solidification process at 0 °C after a quench. Structure evolution as observed in a time-dependent SWAXS experiment.

time demonstrates that a process sets in which is associated with a densification. The absence of any Bragg reflection in the given WAXS patterns comes as expected in view of previous work (Figure 3 in ref 4) which showed for the mesomorphic phase only one broad, halo-like peak at 17° outside the range of our measurement. In the SAXS curve a peak shows up and increases in intensity up to a final value. A first, an interesting result follows directly from the peak position: The associated long spacing, $L = 8$ nm, practically agrees with that found for the semicrystalline structure grown at room temperature. The observation suggests to assume for the mesomorphic phase also a layer structure. We then can further evaluate the data and deduce from the interface distance distribution function

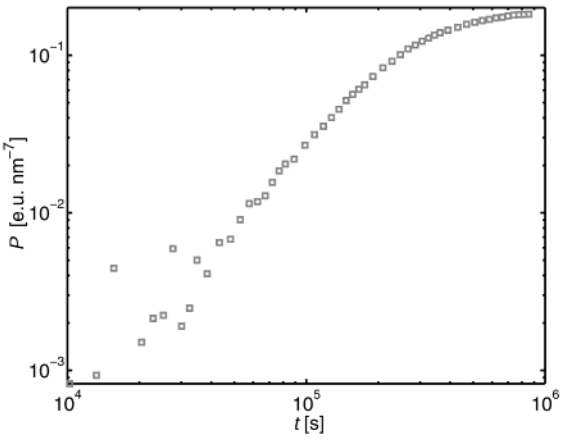

Figure 6. Time dependence of the Porod coefficient as derived from the SAXS data in Figure 5.

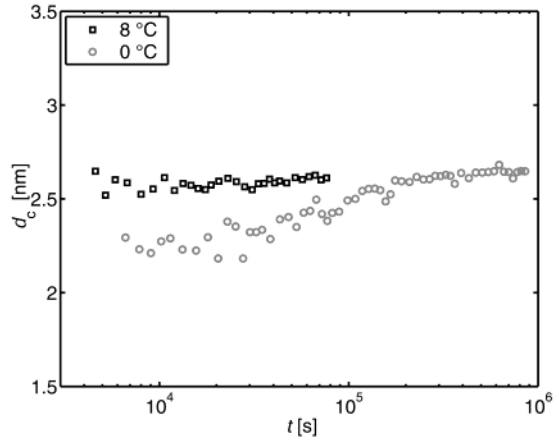

Figure 7. (circle) Time dependence of d_c as derived from the SAXS data in Figure 5. (square) Time dependence of d_c derived from a SAXS experiment carried out at 8for sPP-F.

in the same way as for semicrystalline polymers the Porod coefficient and the layer thickness. Figure 6 displays the time dependence of P associated with this structure formation process. As one notes, the time required to complete the process is in the order of hours. One can compare the final values of P reached for the trans-planar mesomorphic phase and for the semicrystalline phase grown at room temperature. One finds a ratio of 2.5, which yields a factor $\sqrt{2.5} = 1.6$ between the density differences between crystals and fluid amorphous regions and between the trans-planar mesomorphic phase and the fluid.

Figure 7 shows the thickness d_c of the mesomorphic layers, as they were derived from the location of the peak in the IDF for various times in the course of the structure evolution. The first measurement having sufficient intensity to derive an IDF indicated a thickness of 2.2 nm, which then increases up to a final value. The thickness increase is first proportional to log t but then levels off at 2.7 nm. This final value practically agrees with that found for the crystallization at 25 °C. Hence, although the growing layers are definitely noncrystalline, the layer system agrees in its geometrical properties with that created by a crystallization at 25 °C.

The densification shows up also in the dilatometric measurement. Its result is given in Figure 8. As can be noted, the change in the specific volume with time, $\Delta v(t)$, shows the same form as the time dependence of the

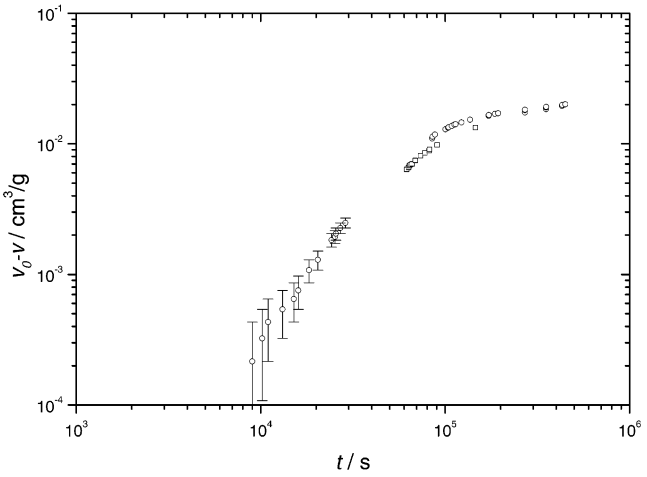

Figure 8. sPP-M: solidification process at 0 °C. Change of the specific volume with time.

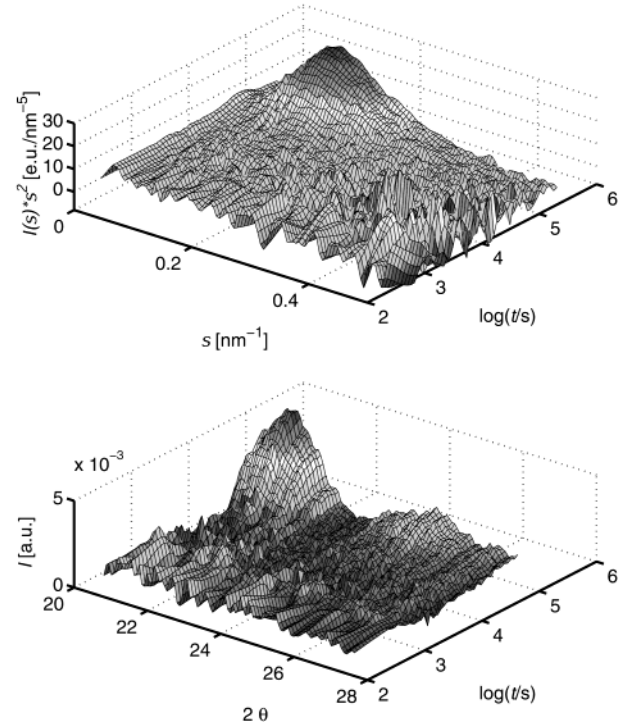

Figure 9. PP-F: solidification process at 2 °C after a quench in ice water. Structure evolution as observed in a time-dependent SWAXS experiment.

Porod coefficient. In particular, both obey during the initial stages a power law

$$\Delta v \sim P \sim t^2 \tag{10}$$

Such a law is indicative for a process where a fixed number of layers grow in the two lateral directions. The agreement of the power-law exponents in the two experiments also tells us that the density difference between the mesomorphic phase, and the melt does not change during the structure evolution. Since P and $v_0 - v$ are proportional to $\Delta\rho^2$ and $\Delta\rho$, respectively, a varying density difference would lead to different exponents.

To demonstrate the difference, Figure 9 displays the SWAXS results obtained for a solidification process carried out at 2, after a short quench in ice−water. In contrast to the observations at 0 °C, now a Bragg

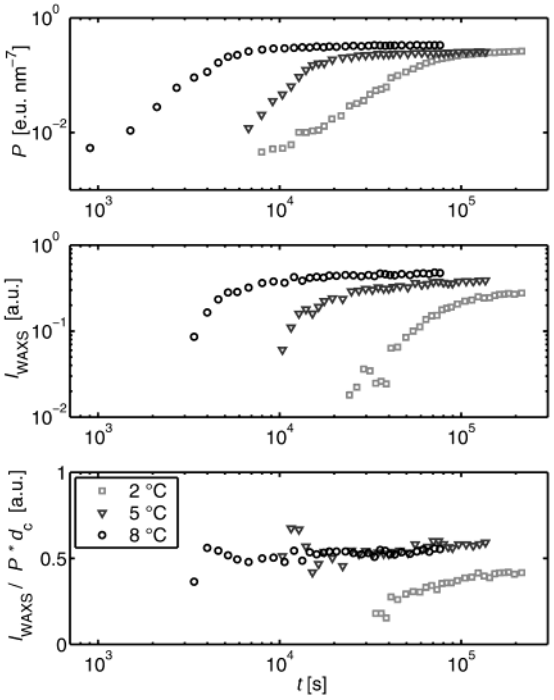

Figure 10. sPP-F, solidified at 2, 5, and 8 °C. Time dependence of the Porod coefficient P (top), the intensity of the wide angle reflection I_{WAXS} (center), and the SWAXS ratio (bottom).

reflection shows up in the course of the structure evolution. SWAXS measurements were also carried out during solidification processes at 5 and 8 °C. Figure 10 collects all results obtained, with the Porod coefficient at the top, the Bragg reflection intensity in the center, and the SWAXS ratio at the bottom, as they develop with time. In addition, the time dependence of the layer thickness as observed at 8 °C is included in Figure 7.

Different from the result at 0 °C, d_c is now constant, thereby agreeing with the final value of the mesomorphic layer. The final value of the Porod coefficient increases with the chosen temperature. The value for 8 °C comes already near to the results found for the semicrystalline phase at room temperature. Of interest is also the result obtained for the SWAXS ratio. We find a constant value for the structure formation at 5 and 8 °C, but deviations associated with a change in time for the structure formation at 2 °C. For this lowest temperature, the final value reached by the SWAXS ratio is also clearly lower.

After the studies of the isothermal kinetics of transformation we investigated in a next step the structure changes during heating processes, performed for both the 0 °C-formed and the 25 °C-formed sample. Figure 11 compares the variations with temperature of the long spacing and the layer thickness: The two measured curves are practically identical. We find a perfect agreement throughout the continuous structure changes which indicate for both samples a continuous melting and re-formation of the layer structure. For the two samples with their definitely different crystallinity the processes take place in an identical manner. The crystallinities of the two samples and their changes with temperature are depicted in the curves presented in Figure 12. They are most clearly reflected in the Bragg intensities given in the center. The large difference which exists at first at room temperature becomes smaller with heating and disappears then for temperatures above 70 °C. Correspondingly, the SWAXS ratio,

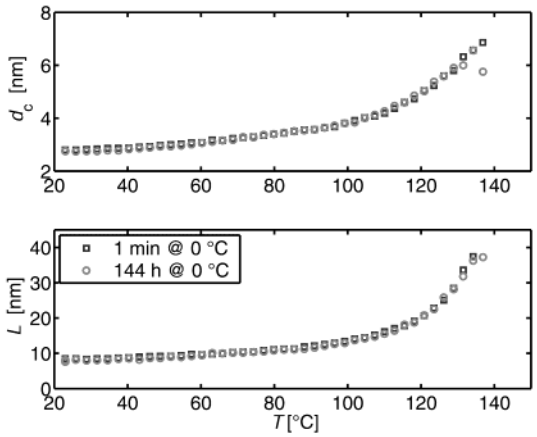

Figure 11. sPP-M, solidified at 0 °C (circle) and crystallized at 25 °C (square). Change of d_c and the long spacing L during a heating from 25 °C to temperatures near to the melting point: Both samples follow identical curves.

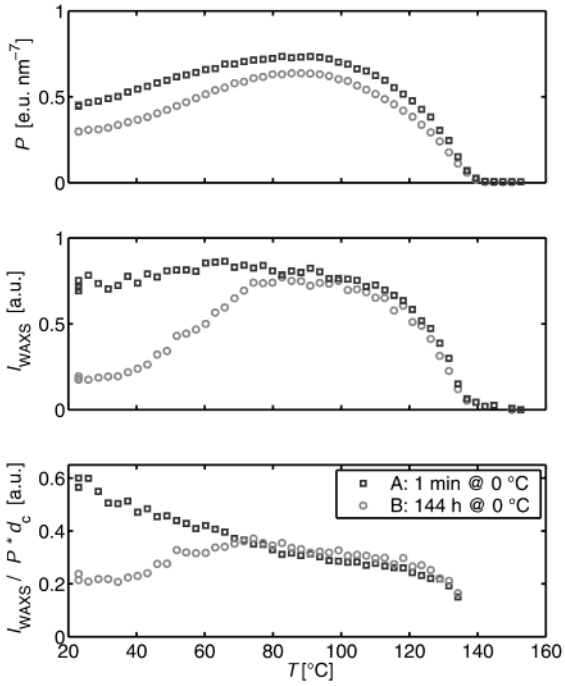

Figure 12. sPP-M, solidified at 0 °C (circle) and crystallized at 25 °C (square). Changes of the Porod coefficient (top), the intensity of the wide angle reflection (center), and the SWAXS ratio (bottom) during a heating to the melt.

being proportional to the fraction of crystalline layers in the layer system, also begins at low values and then increases. The superposed continuous decrease of the ratio in this temperature range is due to the already mentioned increase in the electron density difference in P.

Discussion

How can we understand these results, and this means in particular how can we understand the independence of the structure geometry of the inner layer structure, which can be helical crystalline or trans-planar mesomorphic? We see two different answers: a simple one, which, however, has a problem, and another, at the first glance, a more involved one. The simple view is formation of the trans-mesophase not only takes place at 0 °C but precedes always the crystallization as a first step. It is the trans-mesophase which determines the layer

thickness and the long spacing. The transition into the crystal phase is then a second step which leaves these parameters unchanged. As demonstrated by the heating experiments, this holds not only for isothermal processes but also for the melting−recrystallization processes taking place during a heating. To describe the time dependence of the SWAXS ratio observed for the crystallization at 2 °C, we write for the Porod coefficient

$$P \sim O_{am}(\rho_m - \rho_a)^2 + O_{ac}(\rho_c - \rho_a)^2 \qquad (11)$$

This means that we represent P as being composed of separate contributions by trans-planar mesomorphic and crystalline layers, associated with an interface area per unit volume O_{am} produced by trans-planar mesomorphic layers with a density ρ_m and the analogous quantities O_{ac} and ρ_c for the crystalline layers. The expression can be rewritten as

$$P \sim \frac{1}{d_c}[\phi_m(\rho_m - \rho_a)^2 + \phi_c(\rho_c - \rho_a)^2] \qquad (12)$$

whereby d_c denotes the common layer thickness. As the Bragg intensity is proportional to the crystallinity

$$I_{WAXS} \sim \phi_c \qquad (13)$$

one obtains for the SWAXS ratio the expression

$$\frac{I}{Pd_c} \sim \frac{\phi_c}{\phi_m\left(\frac{\rho_m - \rho_a}{\rho_c - \rho_a}\right)^2 + \phi_c} \qquad (14)$$

The right-hand side of this expression vanishes if all the lamellae are mesomorphic, becomes unity if no trans-planar mesomorphic layers are left, and generally increases with the fraction of crystalline layers in the stacks. Such an increase is observed at 2 °C.

The scheme is simple but includes a problem. As shown by the final value of the SWAXS ratio found for the structure formation at 2 °C, which is below the value reached at the higher temperatures, the transformation from the trans-mesophase to the crystalline phase remains here incomplete. The 0 °C solidified sample is the even more drastic case, as it remains completely mesomorphic when brought to room temperature. One therefore has to ask about the property that prevents part or all of the mesomorphic phase from being transformed into the final crystalline form. We could state that, if this mesomorphic phase exists for long enough time, it becomes in some way stabilized, but this is of course no satisfying answer. In their first discussion of the question, Nakaoki, Ohira, and Horii presented another idea.[2] They found that the fixing of the trans-planar mesomorphic phase after a long storage at 0 °C is in fact not really perfect. A certain fraction, although small, always turns into the crystalline state. This takes place during the transfer from 0 to 25 °C in the range around 12 °C and is associated with a weak endothermal DSC signal. Referring to this observation, the authors proposed that there might exist two different trans-rich phases, the observed stable one and another with a meltlike density and a corresponding higher mobility, which can transform into the crystalline state. Taking up this idea, we go a step further and propose: The first stage in the solidification process of sPP at low temperatures is *always* the formation of a mobile mesomorphic phase. At 0 °C it turns into the observed trans-planar mesomorphic phase; for higher temperatures, above 4 °C, it transforms into the helical crystalline phase. In this view, opposite to the first, simpler scheme, the trans-planar mesomorphic phase is not an intermediate on the way to the crystal phase. It is a modification, although noncrystalline, which is metastable, and has to melt, before crystals can form. Considering the density of the trans-planar mesomorphic phase, which is nearer to the crystalline state than to the melt, a high stability looks conceivable. Of course, introducing another, not directly observable, phase is a complication, but it avoids the mentioned problem. Also, assuming the occurrence of a mobile mesomorphic phase prior to the crystal formation is not new. Various experiments on different systems point in this direction.[9]

Whether the first or the second answer is correct, or still another answer is the right one, cannot be decided at present; however, some conclusion can be drawn:

(i) Not only crystalline but also noncrystalline layers can develop out of a polymer melt, thus building up a rigid skeleton.

(ii) The inner structure of the lamellae with variations in the degree of crystallinity is obviously a secondary property, not related to the selection of the layer thickness and long spacing. This observation is, in any case, indicative for a multistage process in the transformation of the melt into the final solid state.

Acknowledgment. Support of this work by the Deutsche Forschungsgemeinschaft is gratefully acknowledged. Thanks are also due to the Fonds der Chemischen Industrie for financial help.

References and Notes

(1) Nakaoki, T.; Ohira, Y.; Hayasi, H.; Horii, F. *Macromolecules* **1998**, *31*, 2705.
(2) Ohira, Y.; Horii, F.; Nakaoki, T. *Macromolecules* **2000**, *33*, 5566.
(3) Guadagno, L.; D'Aniello, C.; Naddeo, C.; Vittoria, V. *Macromolecules* **2000**, *33*, 6023.
(4) Vittoria, V.; Guadagno, L.; Comotti, A.; Simonutti, R.; Auriemma, F.; De Rosa, C. *Macromolecules* **2000**, *33*, 6200.
(5) De Rosa, C.; Auriemma, F.; Ruiz de Ballesteros, O. *Polymer* **2001**, *42*, 9729.
(6) Ruland, W. *Colloid Polym. Sci.* **1977**, *255*, 417.
(7) Schmidtke, J.; Strobl, G.; Thurn-Albrecht, T. *Macromolecules* **1997**, *30*, 5804.
(8) Hauser, G.; Schmidtke, J.; Strobl, G. *Macromolecules* **1998**, *31*, 6250.
(9) Strobl, G. *Eur. Phys. J. E* **2000**, *3*, 165.
(10) Men, Y.; Strobl, G. *J. Macromol. Sci., Phys.* **2001**, *B40*, 775.

MA021074T